Proc. Natl. Acad. Sci. USA
Vol. 78, No. 2, pp. 676–680, February 1981
Chemistry

Molecular organization in micelles and vesicles

(chain packing/disorder gradient/curved monolayers and bilayers/statistical lattice theory)

KEN A. DILL† AND PAUL J. FLORY

Department of Chemistry, Stanford University, Stanford, California 94305

Contributed by Paul J. Flory, October 17, 1980

ABSTRACT **The configurations of the hydrocarbon chains in micelles are severely constrained by the space-filling requirements of the chain segments, by the continuity of the chains, and by the micellar geometry. A statistical theory that takes full account of these constraints is developed by using a lattice model. The chain ends are deduced to be nonuniformly distributed, with maximal incidence approximately midway between the center of the micelle and the outer surface. Whereas the chain disorder near the outside of the hydrophobic core may approach that of a liquid, crowding of the chains near the core center imposes a degree of order approaching that in a crystal. These results are at variance with the prevailing view that the micellar interior resembles a "liquid hydrocarbon droplet." Also discussed are the effects of curvature on the chain configurations in monolayers and bilayers. It is found, for example, that the "disorder gradients" in inner and outer half-bilayers of small vesicles should be substantially different. Implications of these results are discussed.**

Micelles consisting of amphiphilic chain molecules occur in spherical, cylindrical, or ellipsoidal shapes. The polar heads of the constituent molecules may form the outside surface of the micelle, with the hydrocarbon chains packed inside, or this arrangement may be inverted. Related phases of amphiphilic molecules include planar bilayers, monolayers at an interface, or small unilamellar vesicles in which a bilayer shell surrounds a spherical, solvent-filled cavity. Amphiphilic phases are ubiquitous. They provide the basic structure for biological membranes and bile salts. Their surfactant properties are of widespread importance for detergency, emulsification, lubrication, catalysis, tertiary oil recovery, and drug delivery.

Nonplanar amphiphilic phases, such as micelles and vesicles, exhibit properties that distinguish them from planar monolayers and bilayers. For example, when planar phospholipid bilayers are sonicated to form unilamellar vesicles of small radius, the melting temperature and enthalpy of fusion are lowered (1, 2), the proton NMR linewidth is markedly narrowed (2, 3), the anistropy of the lipid packing is increased (4–6), the susceptibility to attack by phosphodiesterases is enhanced (7), the solubility of small molecules within the bilayer is altered (8), the packing of the two half-bilayers becomes asymmetric (9–11), and the assimilation of proteins is enhanced (12). These effects of curvature appear to have important consequences in various biological systems. High local curvature in membranes is found in mitochondria, microvilli, synaptic vesicles, alveoli, bacterial pili, and spiculated erythrocytes and may play a role in pinocytosis, cell fusion, and drug action (13).

The physical properties of amphiphilic phases depend on the molecular configurations of the hydrocarbon chains packed within them. In spite of intensive study, however, the details of these chain configurations have not heretofore been critically examined. The usual representation of a micelle is shown in Fig. 1*a*; the chains are depicted to be more or less all-*trans*. The space available near the center of the micelle obviously cannot accommodate the chains in the extended conformations shown. Moreover, this simple picture is incompatible with the prevailing presumption that the micellar core has the structure of a "liquid hydrocarbon droplet" (14–18) wherein those bonds of the chains which are in *gauche* configurations are randomly distributed throughout the micellar core.

The molecular organization in the cores of micelles and vesicles, like that within planar bilayers (19), resembles neither the all-*trans* crystalline state of *n*-alkane chains nor the randomly structured liquid state nor even a liquid-crystalline state of intermediate order. It may be likened instead to the "interphase" between crystalline and amorphous regions in a semicrystalline polymer (20). The molecular chains therein are characterized by a gradient of disorder that joins regions of high order and of liquid-like disorder. The proportion of *gauche* bonds varies along the length of a chain as it traverses the interphase layer.

We have recently presented a statistical theory that takes account of the distribution of configurations of the chain molecules occurring in planar monolayers and bilayers (19). In this paper we adapt and apply that theory to the curved geometries incident in micelles and vesicles.

The molecular organization in condensed phases is determined predominantly by short-range repulsive forces between the flexible chains (21, 22). The hydrocarbon chains in micelles and membranes are packed to densities approximating those of corresponding liquids, which are only ≈10% below the density of crystalline *n*-alkanes (2, 23). X-ray diffraction experiments on amphiphilic phases above their melting temperatures reveal a diffuse reflection at 4.6 Å (14, 15), similar to that found in *n*-alkane liquids, which are configurationally disordered (24). Voids are virtually precluded by intermolecular cohesive forces, and molecules of solvent (water) are excluded by so-called hydrophobic interactions. [Anisotropic dispersion forces, sometimes invoked to account for partial molecular order, can be shown to be negligible for hydrocarbon chains (22, 25).]

For the reasons stated, it is a foremost requisite of a suitable model that the hydrocarbon chains be required to fill the space available to them in the micellar core or vesicle bilayer without, however, imposing overlaps between units of neighboring chains (26). Lattice models fulfill these requirements and are particularly convenient for enumeration of molecular configurations. Such models are used for the theory presented below.

Theory

Application of the lattice model to a system of chain molecules requires specification of a segment which, in order to be accommodated by a lattice cell in all orientations, must be equidimensional. Its length is therefore taken to be equal to the mean diameter of the chain. For *n*-alkyl chains, the segment so defined spans ≈3.6 methylene groups. We assume that chain bending

The publication costs of this article were defrayed in part by page charge payment. This article must therefore be hereby marked "*advertisement*" in accordance with 18 U. S. C. §1734 solely to indicate this fact.

† Present address: Department of Chemistry, University of Florida, Gainesville, FL 32611.

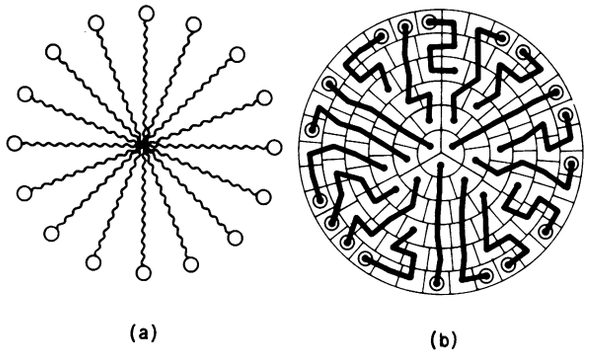

FIG. 1. (*a*) Conventional representation of a micelle. (*b*) Lattice model representation. Because the diagrams are two-dimensional, they most nearly resemble the cross section of a cylindrical micelle.

occurs freely; differences in intramolecular energies of the various configurations are ignored at the level of approximation of the following analysis.

Minimization of the surface free energy requires the polar head groups to be localized at the interface between solvent and the hydrocarbon region. The chains emanating from this interfacial surface penetrate successive layers of the lattice. The number of chains entering a given layer is termed the "chain flux." The continuity of the chains requires that the flux be conserved from one layer of the lattice to the next except as it may be attenuated by termination of chains and by reversal of their directions. For the short chains considered here, reversals may be ignored.

We consider a micelle or a vesicle half-bilayer comprising J_1 chains, each consisting of $n + 1$ segments connected by n flexible bonds. The segments are assigned locations on a three-dimensional curved lattice such that each lattice site accommodates one chain segment. The lattice is constructed so that the radial interlayer spacing is constant; the lattice sites are of equal volume and are approximately isodiametrical (see Fig. 1*b*). In the limit of large radius, the model conforms to the simple cubic lattice. The lattice representation of molecular configurations is artificial. The essential function of the lattice here is to apportion the volume equitably at all radii. As the radius becomes very small, the lattice so defined severely distorts the intersegment distances (i.e., the "bond" lengths). This deficiency is presumed to be of little consequence for our purposes.

The chain segments are numbered sequentially beginning at the heads located at the interface and increasing toward the tails. We examine four cases:

(*i*) *Spherical micelles.* The head groups are arrayed in the first (outermost) shell of a lattice whose layers are arranged radially like those of an onion (see Fig. 1*b*). The flux of chains is radially inward.

(*ii*) *Cylindrical micelles.* The head groups occur in the outermost cylindrical shell; interior layers are arranged concentrically. The chain flux vector is directed radially inward toward the cylinder axis.

(*iii*) *Outer monolayers* such as occur in vesicles and in the amphiphilic interphase of oil-in-water microemulsions. The lattice and the flux direction are the same as in case *i*. However, the radial distance from the center of the sphere to the outer layer of polar heads is greater than the length of the chain.

(*iv*) *Inner monolayers* such as occur in vesicles, inverted micelles, and the interphase of water-in-oil microemulsions. The head groups are located in a layer on the spherical lattice. The chain flux is directed radially outward.

Ellipsoids, inverted cylindrical phases, or other more complicated shapes (27) could be accommodated within the framework of this treatment.

The statistical method for calculating the distribution of chain configurations is the same as previously used (19) for planar bilayers. Let J_i denote the flux of chains from layer $i - 1$ to i. Integrity of the chains requires that

$$J_i = J_{i-1} - T_{i-1}, \qquad [1]$$

in which T_i is the number of chains terminating in layer i. Complete filling of each layer requires that

$$J_i = N_i - R_i, \qquad [2]$$

in which R_i is the number of "redundancies" or lateral placements of segments, and N_i is the number of lattice sites in layer i.

Let p_i denote the probability that a chain segment in layer i is succeeded by a "forward" step into layer $i + 1$; the probability of a "redundant" step in the same layer is denoted by q_i. Assuming that reversals of chain direction can be ignored, we have

$$q_i + p_i = 1. \qquad [3]$$

These probabilities are taken to be independent of the configurations of neighboring bonds of the same chain. They are evaluated *a posteriori*, however, from the self-consistency of the intermolecular constraints (see below).

The probability of a given configuration consists of the product of factors $(q_i^{\nu_i} p_i)$ for each layer penetrated by the given chain, ν_i being the number of redundancies in layer i for that configuration. These probabilities are generated by serial multiplication of the generator matrix (19)

$$\mathbf{G} = \begin{bmatrix} q_1 & p_1 & 0 & 0 & 0 & \dots & 0 & 0 \\ 0 & q_2 & p_2 & 0 & 0 & \dots & 0 & 0 \\ 0 & 0 & q_3 & p_3 & 0 & \dots & 0 & 0 \\ \vdots & & & & & & & \\ 0 & 0 & 0 & 0 & 0 & \dots & q_n & p_n \\ 0 & 0 & 0 & 0 & 0 & \dots & 0 & 1 \end{bmatrix} \qquad [4]$$

The sum of the probabilities for all configurations that terminate in layer i is given by the element $(1, i)$ of $\mathbf{G}^n$. It follows that the fluxes, order parameters, and distributions of chain ends and redundancies may be calculated as before (19):

$$T_i/J_1 = \mathbf{A}_1 \mathbf{G}^n \mathbf{C}_i, \qquad [5]$$

$$J_i/J_1 = 1 - \mathbf{A}_1 \mathbf{G}^n \sum_{j=1}^{i-1} \mathbf{C}_j, \qquad [6]$$

$$R_i/J_1 = \mathbf{A}_1 \left(\frac{\partial \mathbf{G}^n}{\partial \ln q_i} \right) \sum_{j=1}^{n+1} \mathbf{C}_j, \qquad [7]$$

in which $\mathbf{A}_1$ and $\mathbf{C}_i$ are the row and column vectors, each of order $n + 1$, in which the indexed elements (1 and i, respectively) are unity, all others being zero.

Combination of Eq. 2 with Eqs. 5–7 gives

$$\mathbf{A}_1 \left[q_i \frac{\partial \mathbf{G}^n}{\partial q_i} \sum_{j=1}^{n+1} \mathbf{C}_j - \mathbf{G}^n \sum_{j=1}^{i-1} \mathbf{C}_j \right] = (N_i/J_1) - 1, \qquad [8]$$

which can be shown to simplify to

$$\mathbf{A}_1 \mathbf{G}^n \left[q_i \mathbf{C}_i + \sum_{j=1}^{i-1} \mathbf{C}_j \right] = 1 - p_i (N_i/J_1). \qquad [9]$$

Whereas for planar layers the number N_i of lattice sites is the same for all layers, for the systems of interest here the number of sites changes from one layer to the next. This dependence of

N_i on the radial layer number i is given in the following sections.

Finally, we define two order parameters. The first, specifying the average order in layer i, is

$$S_i = (3/2)\langle\cos^2\theta_i\rangle - (1/2) = (3/2)p_i - (1/2), \quad [10]$$

in which θ_i is the angle between the radial axis and the chain axis in that layer. The other order parameter expresses the average order with respect to the radial axis of the kth bond connecting segments k and $k+1$. It corresponds, for example, to the results of NMR quadrupolar splitting measurements on specifically deuterated chains (28). It is given by

$$S_k^* = (3/2)\left[A_1\mathbf{G}^{k-1}\mathbf{G}_p\sum_{j=1}^{n+1}C_j\right] - (1/2), \quad [11]$$

in which $\mathbf{G}_p$ is obtained by replacing all diagonal elements of $\mathbf{G}$ by zero.

Micelles

Consider a spherocylindrical micelle consisting of a cylinder h lattice units in length, $r_0 \leq n+1$ lattice units in radius, and having two hemispherical ends of the same radius. The total number of sites in the associated lattice is

$$N_T = \pi r_0^2[(4/3)r_0 + h] = J_1(n+1). \quad [12]$$

The latter equality is dictated by the requirement that the lattice be filled completely. Constancy of volume of the lattice sites requires the number of sites in the spherocylindrical ith layer to be

$$N_i = \pi\{(4/3)(3[r_0 - i + 1][r_0 - i] + 1) + h(2[r_0 - i] + 1)\}. \quad [13]$$

Thus, when $h \gg r_0$, the micelle is predominantly cylindrical; when $h = 0$, it is spherical. Calculations for these two limiting cases are presented below.

The surface flux density, $\sigma = J_1/N_1$, is fixed by the relationship between r_0 and n through Eqs. 12 and 13. For the calculations presented here, $r_0 = n + 1$. This value of the radius is the maximum for which there is no void at the center; it minimizes the surface-to-volume ratio and is consistent with x-ray diffraction measurements of micellar size (15). In the limit of large chain length, $\sigma \to 1/3$ for spheres and $\sigma \to 1/2$ for long cylinders.

Given n, r_0, and h, Eqs. 12 and 13 may be used to compute J_1/N_i. The values of q_i are then calculated from Eq. 9 consecutively for layers $i = 1,2, \ldots, r_0$.

Results of the calculations for spherical micelles are shown on Fig. 2 *Left*. The flux density of chains is affected by two opposing factors: chain flux (Fig. 2*a*) decreases toward the center due to terminations, but the area also decreases. The terminal ends of the chains (Fig. 2*b*) are distributed broadly throughout the micelle, with a maximum near radius $r = 0.5\,r_0$. This deduction contrasts sharply with the familiar model shown in Fig. 1*a*, which violates density requirements by concentrating the chain ends near $r = 0$. It is also at variance with the liquid hydrocarbon model, according to which the chain ends are uniformly distributed throughout the volume so that the fraction T_i/J_1 of chains terminating in layer i should be proportional to r^2 and, hence, maximal at the outside surface, $r = r_0$.

According to the present analysis, the configurational freedom of the chains is greatest at the outside surface of the micelle, as is shown by profiles of the redundancies (Fig. 2*c*) and by the radial order parameter S_i (Fig. 2*d*).‡ This conclusion holds for any chain length. The order parameter along the chain

‡ Allowance was made (approximately) for the fact that some of the chains must enter the center layer $i = r_0$ at nonzero angle θ_{r_0}.

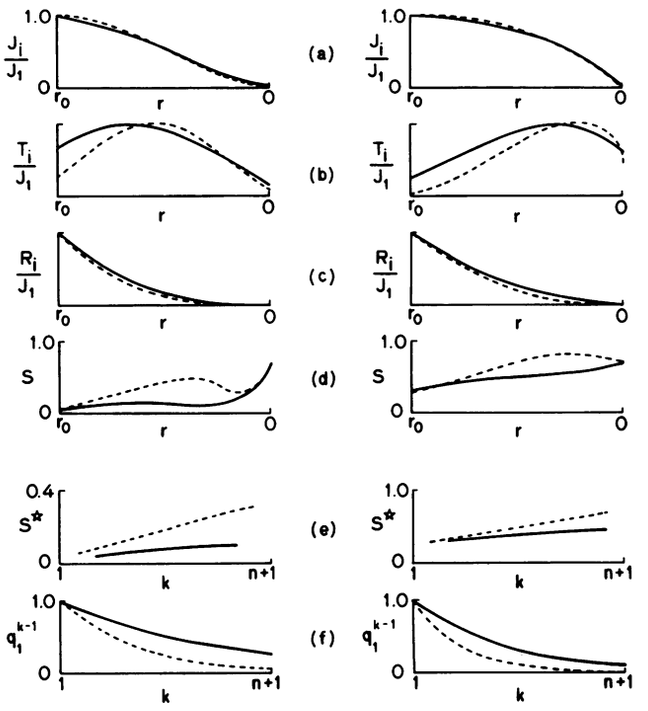

FIG. 2. Results calculated from the lattice theory for spherical (*Left*) and cylindrical (*Right*) micelles. Solid line, $n = 3$; dashed line, $n = 6$. The micellar radius is equal to the chain length, $r_0 = n + 1$. On the abscissas, r is the radial distance from the center of the micelle to the polar heads; k is the chain segment number from the heads toward the tails. The ordinates for b and c are in arbitrary units; they are normalized to give the same areas in b and to give the same values at r_0 for c.

(Fig. 2*e*) also increases near the chain termini. However, the disorder gradient along the chain is not as steep as the radial disorder gradient because very few of the chains sample the deepest parts of the micellar core. Nevertheless, the hydrocarbon core of a spherical micelle is seen to be relatively disordered (liquid-like) on the outside and highly ordered at the center.

Fig. 2 *Right* shows the corresponding results for cylindrical micelles. The chain configurations in cylindrical micelles closely resemble those in spherical micelles; the minor differences are in the direction of a closer correspondence to planar chain packing. For cylinders, regardless of size, the degree of order is substantially greater near the center than at the outisde. Differences in chain configurations between cylindrical and spherical geometries follow directly from the respective dependences of the area per chain (inversely, the chain flux density) on the radius. The preferred location of the chain termini is nearer $r = 0$ than for spheres. Also, the gradient of disorder is less pronounced. The predictions that micellar structures are generally disordered and that they are less so in cylindrical systems are supported by laser Raman scattering experiments (29). The chain configurations in micelles of prolate and oblate ellipsoids may be presumed to resemble those of the cylindrical and planar cases, respectively, for large asymmetry, and spheres for small asymmetry. Also, if the radius of a micelle of any shape is smaller than the chain length (i.e., if $r_0 < n + 1$), then the disorder must be greater throughout the micelle than in the examples presented with $r_0 = n + 1$.

The proposed model for micellar structure resolves several paradoxes.

(*i*) In reviewing the subject, Menger (16) states, "Difficulties in devising a satisfactory micelle model originate not so much from a paucity of experimental data but rather from conflicting

conclusions based on that data. Consider the viscosity of the micelle core. . . ." Experiments using various probes (NMR, fluorescence, and electron spin resonance) yield conflicting results. Some indicate a solid micelle interior, others a liquid interior (for reviews, see refs. 14–17). Our analysis suggests that the structure monitored by the probe depends on the depth to which it penetrates. Deeply embedded probes should register a solid structure, and superficially embedded ones should indicate a liquid environment. Indeed, when pyrene (30), 2-methylanthracene (31), or sterol nitroxide (32) probes are used, all of which are large rigid molecules with the potential to penetrate the solid core of the micelle, the measured anisotropies are high. Low anisotropies, on the other hand, are measured by a small polar nitroxide biradical (33), which probably localizes near the micelle–solvent interface, and by a terminal benzene probe on a flexible alkane (34), which may be distributed throughout the same broad liquid environment as the chain ends of the constituent micellar alkanes. For a spherical micelle composed of 14-carbon chains ($n + 1 \cong 4$), the order parameter S_4^* for the terminal methyls is approximately 0.1 (see Fig. 2*e*), implying that its environment is almost liquidlike. It should be noted that the degree of internal anisotropy is sensitive also to the radius and shape of the micelle (see Fig. 2 *d* and *e*). Dynamic measurements, such as NMR T1 relaxations, have both orientational and kinetic components (35) and, therefore, cannot be interpreted in terms of configurational theories such as the one presented here.

(*ii*) Menger states further, "Water penetration into the micelles, a critically important matter in micellar structure, suffers from the same bewildering array of opinions as micellar viscosity . . . " (ref. 16; see also refs. 17, 18, and 36). Spectroscopic evidence from a variety of studies indicates "hydration" of the first few methylene groups near the polar heads. This has been taken as evidence for the penetration of water into the micellar core, causing a surface "roughness" (16, 37). The present theory offers an alternative explanation. Consistent with an observation of Wennerström and Lindman (36) is the idea that spectroscopic methods measure the proximity of the probe to water, interfacial or internal, whereas measurements of thermodynamic and transport properties measure only the amount of water bound internally in the core. The latter experiments show no evidence for water penetration. Therefore, only those probes attached to chain segments in the outermost layer of the micelle register close proximity to the solvent. The probability that a chain segment k is located in the first lattice layer is q_1^{k-1}. This quantity is plotted in Fig. 2*f*. Indeed, it can be seen that for a 14-carbon chain in a spherical micelle there is a substantial probability that a methylene group even halfway down the chain may occur in the outermost layer of the lattice; this is consistent with spectroscopic results (14–17, 36). Furthermore, some few chains are predicted to lie entirely on the outside layer of the micelle so that even their termini reside near the interface.

(*iii*) Finally, ". . . one must ask why many water-insoluble compounds (e.g., benzophenone, bromobenzene, butyronitrile) apparently prefer the highly aqueous micelle surface to the organic interior" (16). Our results suggest that the preference of these hydrophobic solutes may not be for the surface *per se*, but rather for the disordered outer region of the micellar core. The solubility is expected to be greater in the outer liquid core than in the inner ordered core because the disordered region affords a greater configurational entropy of mixing. The degree of chain ordering affects the solubility of small molecules; for planar bilayer membranes, similar solutes are often more soluble in the disordered L_α phase than in the crystalline phases (14).

The theory developed here is thus consistent with the various measurements of internal viscosity, with the association of water with the micellar hydrocarbon chains and with the selective partitioning of small hydrophobic molecules into the outer liquidlike portion of the micellar core.

Nonplanar monolayers

Monolayers with curvature constitute the inner and outer half-bilayers of vesicles, the amphiphilic interphases in microemulsions, and so-called inverted micelles. Such a monolayer is characterized by the number, $n + 1$, of segments of its constituent chains, by its surface flux density, $\sigma = J_1/N_1$, and by the radius of curvature of its polar interface, r_0 for the outermost shell of an outside monolayer and r_{in} for the innermost shell of an inside monolayer. Given n, σ, and r_0 for an outer monolayer, Eq. **9** is solved consecutively for layers $i = 1,2, \ldots, L$ subject to the geometric requirements that

$$N_i = (4\pi/3)[3(r_0 - i + 1)(r_0 - i) + 1] \quad [14]$$

and $J_1/N_i = \sigma(N_1/N_i)$. The layer number of the last completely filled shell is L, which is determined by

$$\sum_{j=1}^{L} N_j \leq J_1 (n + 1) < \sum_{j=1}^{L+1} N_j. \quad [15]$$

For an inner monolayer, the procedure is the same as above, except that the number of lattice sites per layer is given by

$$N_i = (4\pi/3)[3(r_{in} + i - 3)(r_{in} + i) + 7] \quad [16]$$

rather than by Eq. **14**.

The results of these calculations on the half-bilayers of vesicles are shown in Fig. 3. For large radius of curvature, the structure approaches that of the planar bilayer in which the disorder gradients of the monolayers are symmetric. However, for small radii such as characterize sonicated unilamellar vesicles, the chain packing in the inner and outer monolayers is asymmetric. In particular, the inner monolayer exhibits a steeper disorder gradient than the planar monolayer; this is a consequence of the decrease of chain flux density, radially outward, due to terminations and to a corresponding increase in area. The outer monolayer, on the other hand, adopts some of the inverted disorder gradient characteristic of micelles, and this is superimposed on the planar disorder profile.

These deductions agree with the following experimental results. A packing asymmetry of the chains in inner and outer half-bilayers has been found by Longmuir and Dahlquist (4) by ^{19}F NMR. Furthermore, by the elegant ^{31}P NMR and hydrody-

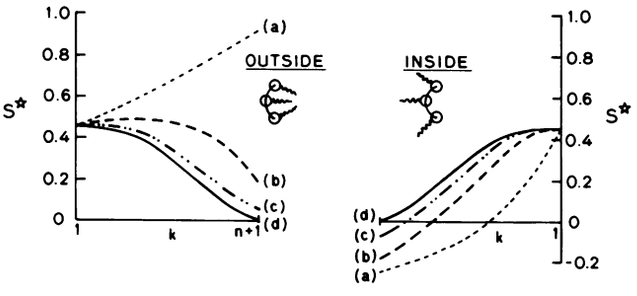

FIG. 3. Bilayers of different radii of curvature; disorder gradients along the chains of inside and outside monolayers; $\sigma = 0.64$ and $n \doteq 4$ throughout; k is the chain segment number. The values of r_0 and r_{in} correspond approximately to monolayers matched to form bilayers. Curves a, $r_0/(n + 1) = 2$; $r_{in}/(n + 1) = 0.8$. Curves b, $r_0/(n + 1) = 4$; $r_{in}/(n + 1) = 2.8$. Curves c, $r_0/(n + 1) = 16$; $r_{in}/(n + 1) = 14.8$. Curves d, $r_0 = r_{in} = \infty$. Comparison of curves c and d shows that there is a considerable deviation from planar packing, even for vesicles as large as ≃700 Å in diameter.

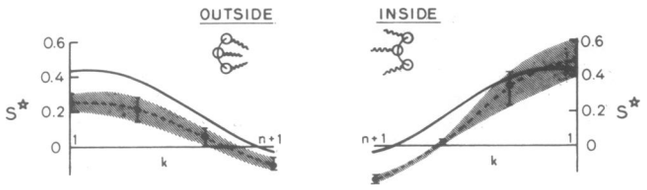

FIG. 4. Asymmetry of half-bilayers in small unilamellar vesicles. The shaded region represents the range of S^* values predicted from measured σ values (9–11). For comparison, the heavy line represents dipalmitoyl lecithin bilayers at 41°C (19).

namic method of Chrzeszczyk *et al.* (9), the area per chain has been shown to differ depending on whether the chains are in a planar bilayer or in the inner or outer monolayers of small lecithin vesicles (9–11). By using the values of chain flux taken from these three studies (9–11), we have calculated the range of expected disorder gradients. They are shown in Fig. 4. For comparison, the predicted disorder gradient for planar dipalmitoyl lecithin bilayers with $\sigma = 0.63$ (19) is also shown. The predictions can be compared with experimental results of Stockton *et al.* (38), who studied the disorder gradient in small vesicles by ^{2}H NMR. The chains were deuterated at specific positions but were symmetrically distributed in both monolayers. They found the disorder at midbilayer to be greater in vesicles than in planar systems; this is consistent with results in Fig. 4. Their further observation that the disorder near the heads is the same as in planar bilayers is consistent with the deduction, shown in Fig. 4, that the tight chain packing inside and the loose chain packing outside give an average that resembles planar packing. The results in Fig. 4 also imply that the net disorder is greater in the vesicle than in the planar bilayer; there is much experimental evidence to support this deduction (4–6). However, such comparisons should be made with caution; the validity of comparing results from egg lecithin with results from synthetic dipalmitoyl phosphatidylcholine systems, and of results for narrow size distributions with those for broader ones, is questionable (6, 39).

We thank Wayne Hubbell and Charlie Springer for helpful discussions and for drawing our attention to some of the references cited. We also benefited from discussions with Michael Brown, Sunney Chan, Leo Neuringer, and Barry Sears. We acknowledge, with thanks, postdoctoral support to K.A.D. from the Damon Runyon–Walter Winchell Cancer Fund, Fellowship DRG-271-F. This work was also supported by the National Science Foundation, Polymers Program, Grant DMR-80-06624.

1. Suurkuusk, J., Lentz, B. R., Barenholz, Y., Biltonen, R. L. & Thompson, T. E. (1976) *Biochemistry* **15**, 1393–1401.
2. Sheetz, M. P. & Chan, S. I. (1972) *Biochemistry* **11**, 4573–4581.
3. Penkett, S. A., Flook, A. G. & Chapman, D. (1968) *Chem. Phys. Lipids* **2**, 273–290.
4. Longmuir, K. J. & Dahlquist, F. W. (1976) *Proc. Natl. Acad. Sci. USA* **73**, 2716–2719.
5. Lentz, B. R., Barenholz, Y. & Thompson, T. E. (1976) *Biochemistry* **15**, 4529–4536.
6. Gaber, B. P. & Peticolas, W. L. (1977) *Biochim. Biophys. Acta* **465**, 260–274.
7. Wilschut, J. C., Regts, J., Westenberg, H. & Scherphof, G. (1978) *Biochim. Biophys. Acta* **508**, 185–196.
8. Huang, C. H., Sipe, J. P., Chow, S. T. & Martin, R. B. (1974) *Proc. Natl. Acad. Sci. USA* **71**, 359–362.
9. Chrzeszczyk, A., Wishnia, A. & Springer, C. S. (1977) *Biochim. Biophys. Acta* **470**, 161–169.
10. Huang, C. & Mason, J. T. (1978) *Proc. Natl. Acad. Sci. USA* **75**, 308–310.
11. Cornell, B. A., Middlehurst, J. & Separovic, F. (1980) *Biochim. Biophys. Acta* **598**, 405–410.
12. Eytan, G. D. & Broza, R. (1978) *FEBS Lett.* **85**, 175–178.
13. Sheetz, M. P. & Singer, S. J. (1974) *Proc. Natl. Acad. Sci. USA* **71**, 4457–4461.
14. Tanford, C. (1980) *The Hydrophobic Effect* (Wiley-Interscience, New York), 2nd Ed.
15. Fendler, J. H. & Fendler, E. J. (1975) *Catalysis in Micellar and Macromolecular Systems* (Academic, New York).
16. Menger, F. M. (1979) *Acc. Chem. Res.* **12**, 111–117.
17. Fisher, L. R. & Oakenfull, D. G. (1977) *Chem. Soc. Rev.* **6**, 25–42.
18. Wennerström, H. & Lindman, B. (1979) *Phys. Rep.* **52**, 1–86.
19. Dill, K. A. & Flory, P. J. (1980) *Proc. Natl. Acad. Sci. USA* **77**, 3115–3119.
20. deGennes, P. (1974) *Phys. Lett. A* **47**, 123–124.
21. Barker, J. A. & Henderson, D. (1972) *Annu. Rev. Phys. Chem.* **23**, 439–484.
22. Wulf, A. (1975) *J. Chem. Phys.* **64**, 104–109.
23. Nagle, J. F. & Wilkinson, D. A. (1978) *Biophys. J.* **23**, 159–175.
24. Flory, P. J. (1979) *Faraday Discuss. Chem. Soc.* **68**, 14.
25. Warner, M. (1980) *J. Chem. Phys.* **73**, 5874.
26. Scott, H. L. & Cherng, S. L. (1978) *Biochim. Biophys. Acta* **510**, 209–215.
27. Israelachvili, J. N., Mitchell, D. J. & Ninham, B. W. (1976) *J. Chem. Soc. Faraday Trans. 2* **72**, 1525–1568.
28. Seelig, J. (1977) *Q. Rev. Biophys.* **10**, 353–418.
29. Kalyanasundaram, K. & Thomas, J. K. (1976) *J. Phys. Chem.* **80**, 1462–1473.
30. Pownall, H. J. & Smith, L. C. (1973) *J. Am. Chem. Soc.* **95**, 3136–3140.
31. Shinitzky, M., Dianoux, A. C., Gitler, C. & Weber, G. (1971) *Biochemistry* **10**, 2106–2113.
32. Povich, M. J., Mann, J. A. & Kawamoto, A. (1972) *J. Colloid Interface Sci.* **41**, 145–147.
33. Ohnishi, S., Cyr, T. J. R. & Fukushima, H. (1970) *Bull. Chem. Soc. Jpn.* **43**, 673–676.
34. Menger, F. M. & Jerkunica, J. M. (1978) *J. Am. Chem. Soc.* **100**, 688–691.
35. Brown, M. F. (1979) *J. Magn. Reson.* **35**, 203–215.
36. Wennerström, H. & Lindman, B. (1979) *J. Phys. Chem.* **83**, 2931–2932.
37. Stigter, D. & Mysels, K. J. (1955) *J. Phys. Chem.* **59**, 45–51.
38. Stockton, G. W., Polnaszek, C. F., Tulloch, A. P., Hasan, F. & Smith, I. C. P. (1976) *Biochemistry* **15**, 954–966.
39. Mendelsohn, R., Sunder, S. & Bernstein, H. J. (1976) *Biochim. Biophys. Acta* **419**, 563–569.